The EMBO Journal vol.13 no.2 pp.327-337, 1994

The active site of yeast aspartyl-tRNA synthetase: structural and functional aspects of the aminoacylation reaction

Jean Cavarelli, Gilbert Eriani[1], Bernard Rees, Marc Ruff, Marcel Boeglin, André Mitschler, Franck Martin[1], Jean Gangloff[1], Jean-Claude Thierry and Dino Moras[2]

UPR 9004, Laboratoire de Biologie Structurale and [1]UPR 9002, Structure des Macromolécules Biologiques et Mécanismes de Reconnaissance, Institut de Biologie Moléculaire et Cellulaire du CNRS, 15 rue René Descartes, 67084 Strasbourg Cedex, France
[2]Corresponding author

Communicated by D.Moras

The crystal structures of the various complexes formed by yeast aspartyl-tRNA synthetase (AspRS) and its substrates provide snapshots of the active site corresponding to different steps of the aminoacylation reaction. Native crystals of the binary complex tRNA-AspRS were soaked in solutions containing the two other substrates, ATP (or its analog AMPPcP) and aspartic acid. When all substrates are present in the crystal, this leads to the formation of the aspartyl-adenylate and/or the aspartyl-tRNA. A class II-specific pathway for the aminoacylation reaction is proposed which explains the known functional differences between the two classes while preserving a common framework. Extended signature sequences characteristic of class II aaRS (motifs 2 and 3) constitute the basic functional unit. The ATP molecule adopts a bent conformation, stabilized by the invariant Arg531 of motif 3 and a magnesium ion coordinated to the pyrophosphate group and to two class-invariant acidic residues. The aspartic acid substrate is positioned by a class II invariant acidic residue, Asp342, interacting with the amino group and by amino acids conserved in the aspartyl synthetase family. The amino acids in contact with the substrates have been probed by site-directed mutagenesis for their functional implication.
Key words: aminoacylation/aspartyl-tRNA synthetase/ ATP/crystal structure/tRNA

Introduction

Aminoacyl-tRNA synthetases (aaRS) are responsible for the specific aminoacylation of transfer RNAs (Schimmel, 1987). Each of the 20 aaRS, one for each amino acid, catalyzes a two-step reaction which involves three substrates (ATP, amino acid and tRNA) (Schimmel, 1987; Lapointe and Giegé, 1991; Söll, 1991). The first step is the activation of the amino acid with the formation of an aminoacyl-adenylate intermediate in the presence of magnesium ions. The second step is the transfer of the amino acid moiety from the adenylate to the terminal ribose of tRNA. Except in GluRS, GlnRS and ArgRS, the first step does not require the presence of the cognate tRNA (Schimmel and Söll, 1979).

This family of enzymes can be partitioned into two classes according to structural features detected by primary sequence analysis (Eriani *et al.*, 1990) and visualized by crystallography (Cusack *et al.*, 1990; Ruff *et al.*, 1991). All class I synthetases possess two signature peptides (HIGH and KMSKS) (Hountondji *et al.*, 1986; Burbaum *et al.*, 1990), both located in the active site domain with its characteristic 'Rossmann fold' (Rossmann *et al.*, 1974). The active site domain of class II enzymes exhibits an original fold constituted by a six-stranded antiparallel β-sheet flanked by an additional parallel strand and two α-helices (Cusack *et al.*, 1990; Ruff *et al.*, 1991). The three common signature motifs of this class belong to this domain. The class partition is correlated with a catalytic difference in these enzymes, namely the primary site of attachment of the amino acid to the terminal adenosine. All class I aaRS attach their amino acid to the 2′ hydroxyl group, whereas class II aaRS (with the exception of PheRS) bind their amino acid to the 3′ hydroxyl group of the ribose of the terminal adenosine (Eriani *et al.*, 1990).

A full description of three class I aaRS [MetRS (Brunie *et al.*, 1990), TyrRS (Brick *et al.*, 1989) and GlnRS (Rould *et al.*, 1989, 1991)] and two members of class II [SerRS (Cusack *et al.*, 1990) and AspRS (Ruff *et al.*, 1991; Cavarelli *et al.*, 1993)] has been obtained from their crystal structure. In addition, GlnRS and AspRS provided the first pictures of aaRS bound to their cognate tRNAs along with the first details of tRNA-aaRS interaction at atomic resolution. However, information concerning the active site, especially the binding of ATP and the amino acid, remains scarce. The structure of TyrRS was solved in the presence of tyrosyl adenylate or of the inhibitor tyrosinyl adenylate. The structure-function relationship in TyrRS has been extensively studied by site-directed mutagenesis to uncover atomic interactions involved in catalysis (Fersht, 1987; Fersht *et al.*, 1988; de Prat Gay *et al.*, 1993). GlnRS was solved and refined in the presence of ATP and tRNA. Soaking of crystals in a solution of glutamine resulted in the elimination of pyrophosphate, as shown by the electron density maps, but the glutamine substrate could not be localized. A catalytic mechanism for the aminoacylation by GlnRS was recently proposed (Perona *et al.*, 1993), based on the crystal structure of the complex and on the modelization of the amino acid substrate. In this paper we present the active site of yeast aspartyl-tRNA synthetase in the presence of all its three substrates: the amino acid, ATP and tRNA. Based on the crystallographic results, we propose a mechanism for the aminoacylation reaction. The role of the residues in the binding site pocket has been investigated by site-directed mutagenesis experiments.

To localize the different substrates involved in the aminoacylation reaction and characterize the mechanism of their binding to the synthetase, four independent crystal structures have been studied and refined: the structure of the binary complex between $tRNA^{Asp}$ and the aspartyl-tRNA synthetase; two structures of the ternary complex, with

Table I. Crystallographic data

Crystal	Native	Native soaked with AMPPCP	Native soaked with ATP	Native soaked with ATP and aspartic acid
Data collection				
Resolution limit (Å)	2.7	3.2	3.0	3.0
Observed reflections	32 7516	12 6128	13 5407	20 1793
Unique reflections (F/ sig(F) > 1)	67 061	41 905	46 698	42 727
R_{sym}[a]	0.09	0.087	0.088	0.087
Completeness (%)	90	95	87	80
Structure refinement				
Resolution (Å)	2.9	–	3.0	3.0
Reflections used (F/ sig(F) > 3)	49 370	–	38 665	38 243
R-factor[b]	0.225	–	0.203	0.212
r.m.s. bonds	0.010	–	0.012	0.011
r.m.s. angles (°)	1.8	–	2.3	2.3
Mean B-factor (A^2)	30	–	30	30

[a]$R_{sym} = \Sigma_{hkl} \Sigma_{obs} |I_{obs} - <I>_{hkl}| / \Sigma_{hkl} \Sigma_{obs} I_{hkl}$
[b]R-factor $= \Sigma_{hkl} |F_{obs} - F_{calc}| / \Sigma_{hkl} F_{obs}$
I_{obs} = measured diffraction intensity and $<I>_{hkl}$ = mean value of all intensity measurements of reflection hkl.
F_{obs} = observed modulus and F_{calc} = calculated modulus for the structure factor of reflection hkl.

ATP or with the analog inhibitor AMPPcP; and finally the structure of the complex with ATP and the aspartic acid substrate (Table I). Crystals, prepared as described previously (Ruff *et al.*, 1988), were soaked in solutions of the different substrates without significant loss of diffracting power. They all diffract to ~3 Å resolution or slightly higher.

Results

The active site

Figure 1 shows a stereo view of the active site of AspRS as seen in the crystal structures of the functional ternary complex. The six-stranded antiparallel β-sheet, completed by a seventh parallel strand, constitutes the floor of the active site pocket, whose entrance is half closed by several loops. The ATP molecule lies on the β-sheet giving rise to two cavities. The left-hand cavity is made by the insertion domains between motifs 2 and 3, which include α-helical parts and the last strands of the antiparallel sheet. The right-hand cavity is the amino acid binding pocket, essentially constituted by residues from the conserved motifs. It is narrower but accessible to the amino acid, even with the ATP and CCA in place. The CCA end of the tRNA is positioned on top of the two other substrates.

The surface of the antiparallel β-sheet in contact with the ATP is characterized by an unusually large number of glycine residues (positions 340, 482, 524, 526 and 528). They allow the formation of a cavity with only a few important side chains pointing towards the ATP. These glycine residues are invariant in all sequenced AspRS (with the exception of Gly526, replaced by the short side chain alanine in prokaryotic aaRS and Gly340, replaced in all prokaryotic enzymes by a Gln). Gly528, close to the ribose of ATP, is conserved in almost all sequenced class II synthetases. Any side chain at this position would be unfavorably stacked between the adenine moiety of ATP and Phe338. This structural role of the glycines in a β-sheet can be compared with the situation in the cyclic AMP kinase, where a similar glycine-rich β-sheet peptide constitutes the binding site for the ATP phosphates (Bossemeyer *et al.*, 1993). Several glycines are also observed on the loops at the entrance of the active site, in particular the essentially conserved Gly500, Gly282 and Gly283 (again replaced by Ala in prokaryotes).

A class-specific ATP binding site

The present 3D structures of the complex provide new information on the binding of ATP or its analog AMPPcP in the presence of tRNA, with and without the amino acid substrate. A stereo view of the ATP binding site is shown in Figure 2A. The adenine base of ATP is firmly held by π-electron interactions with Phe338 on one side and Arg531 on the other. The benzene ring and the guanidinium group are parallel to and equidistant (at ~3.5 Å) from the adenine plane. The adenine base is bound to the enzyme by two hydrogen bonds with the main chain carbonyl and nitrogen atoms of Met335. The second main anchoring point of ATP is the α-phosphate which forms a salt bridge with Arg325, a strictly invariant class II residue. Arg531, also conserved in all class II synthetases, interacts also with the γ-phosphate of the ATP. The hydroxyl groups of the ribose are involved in hydrogen bonds with main chain atoms of Ile479 and Gly528. Note that (i) most residues involved in those interactions are part of motifs 2 and 3 and (ii) the residues that interact through their side chains are invariant in all class II synthetases (with the sole exception of Arg325, replaced by a histidine in *Escherichia coli* AlaRS).

Figure 2B and C shows the electron density for the ATP and AMPPcP molecules in the active site. The ATP analog adopts an elongated conformation while the ATP itself is bent. The adenosine moiety and the α-phosphate occupy the same position in both cases, so that the conformational change may be described essentially as a rotation around the bond connecting the α-phosphate to the pyrophosphate group. The bent conformation is stabilized by the presence of a Mg^{2+} ion necessary for the first step of the aminoacylation reaction. The position of this ion is that of

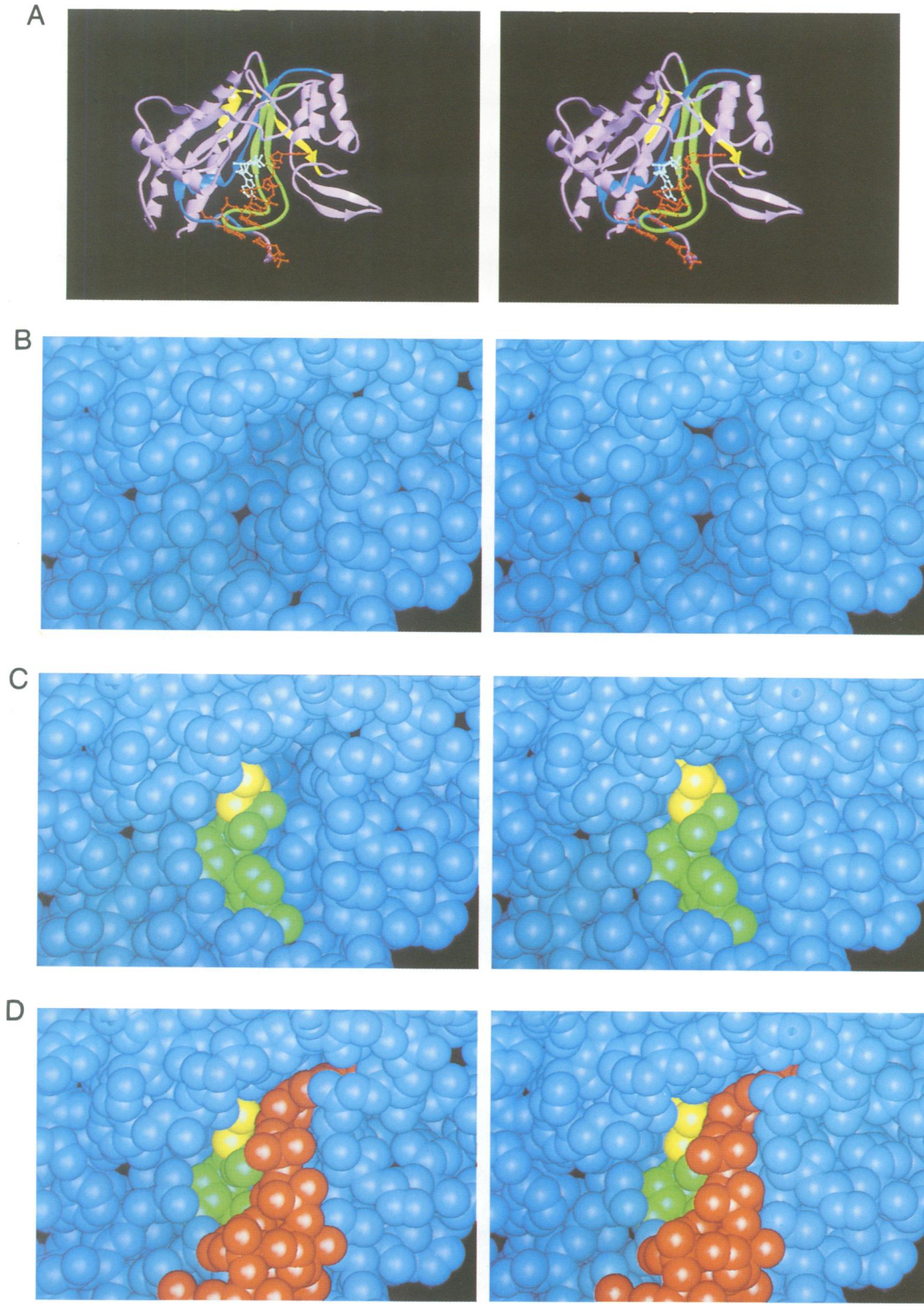

Fig. 1. (**A**) A schematic stereo view of the active site [program RIBBONS (Carson, 1991)], showing the enzyme, the ATP (white) and the acceptor end of tRNA (red). The three motifs conserved in class II synthetases are in yellow (motif 1), green (motif 2) and blue (motif 3). (**B**–**D**) The atoms are shown as hard spheres (Jones and Thirup, 1986). (B) The enzyme active site pocket before fixation of the substrates; (C) the enzyme with an adenylate moiety (AMP is green, the amino acid is yellow); (D) with the tRNA (red). The terminal adenosine base is seen half buried at the upper part of the figure.

a strong peak in the residual electron density located between the β- and γ-phosphates and two conserved amino acid side chains, Asp471 and Glu478.

In AMPPcP, the oxygen linking the β- and γ-phosphates is replaced by a methylene group. The resulting perturbation of the interaction with Mg^{2+} may be the reason for the different conformation adopted by this analog. In the linear conformation (AMPPcP), the γ-phosphate interacts with Arg485, Gln303 and Tyr456 in the pocket which will be occupied by the amino acid substrate (see below). The way the adenine base is secured makes it easy to imagine the possible swinging of the pyrophosphate group around the

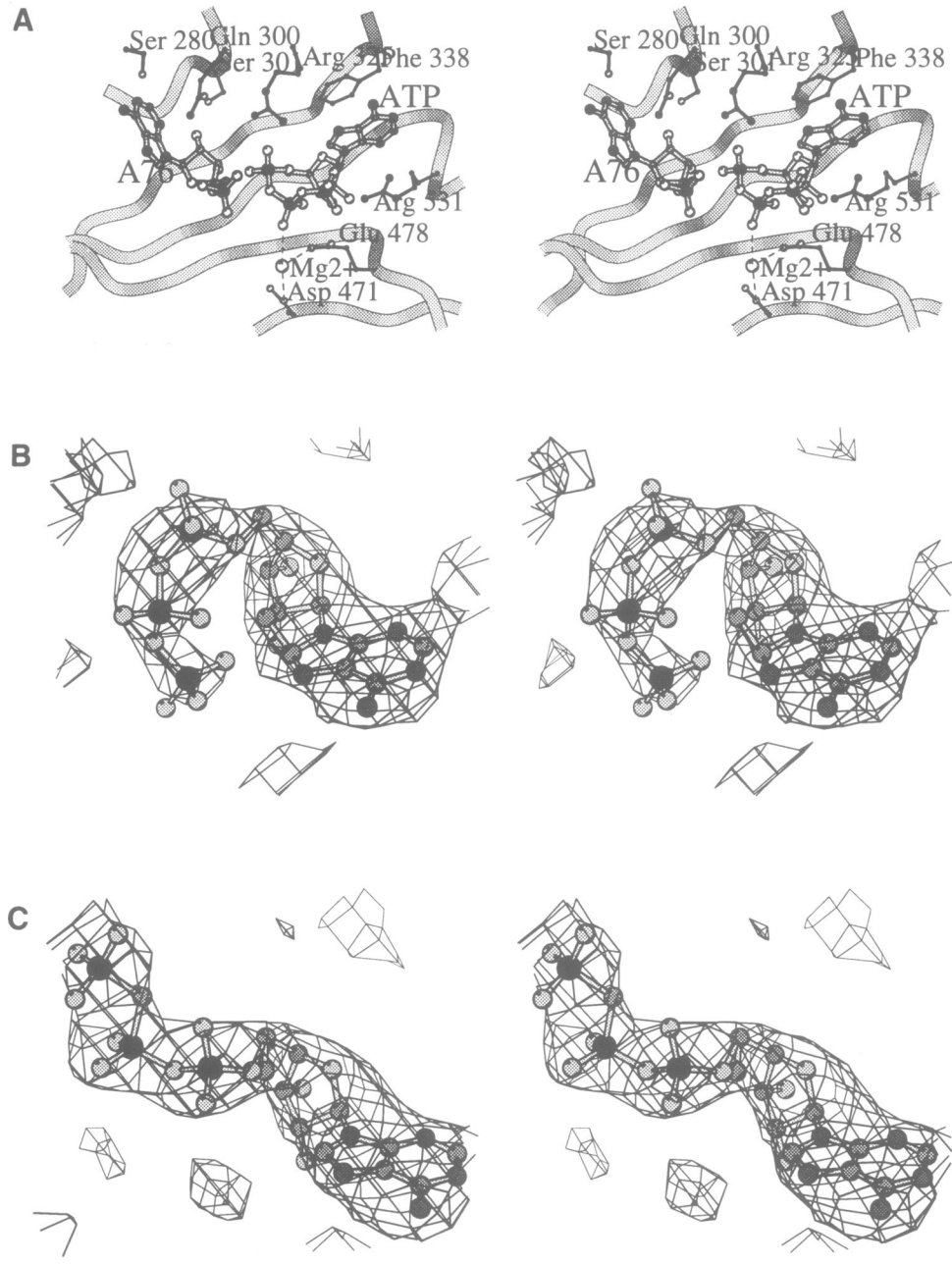

Fig. 2. (**A**) The ATP binding site; (**B**) residual density in the ATP region (crystals soaked with ATP); (**C**) residual density in crystals soaked with the analog AMPPcP. The density maps shown are omit maps (observed − calculated density) where the model used to calculate the density does not include the ATP or its analog. The maps are contoured at the 2.5σ level (i.e. 2.5 times the r.m.s. density of the map). ATP and its analog adopt different conformations, probably because of different interactions with a Mg^{2+} ion. This and all other black-and-white stereo pictures were made using the program MOLSCRIPT (Kraulis, 1991). Electron density is displayed using the program MINIMAGE (J.Arnez, submitted).

bond with the α-phosphate, thus making room for the amino acid substrate.

CCA binding site

The ATP occupies the bottom of the active site in contact with the anti-parallel β-sheet. The CCA extremity of the tRNA lies on top of the ATP and makes contacts essentially with the helices and loops closing the active site pocket (Figure 3). The variable loop of motif 2, from residues 327 to 334, interacts with the amino acid acceptor end of the tRNA from A72 to C75, in particular with the discriminator base G73 (Cavarelli *et al.*, 1993). Two other loops (280−284 and 300−301) make contacts with C75 and A76 (see details in Table II). These loops are all on the same side of the acceptor arm of tRNA. On the other side there are no contacts from the ribose of G73 to the phosphate of A76. This leaves a cleft large enough for the passage of an ATP and an aspartic acid molecule. It is probably of biological importance that the ATP and the tRNA are able to fix (or free) themselves in any order in the active site.

While ATP is bound essentially through class II-specific interactions, most of the residues involved in contacts with the CCA are characteristic of the aspartic acid system and therefore invariant only in the AspRS family, in some cases restricted to the eukaryotes. In this region, only two amino acids are conserved within class II synthetases: His334 (replaced by arginine in some systems), which makes the only observed interaction with the base of C75, and Glu327

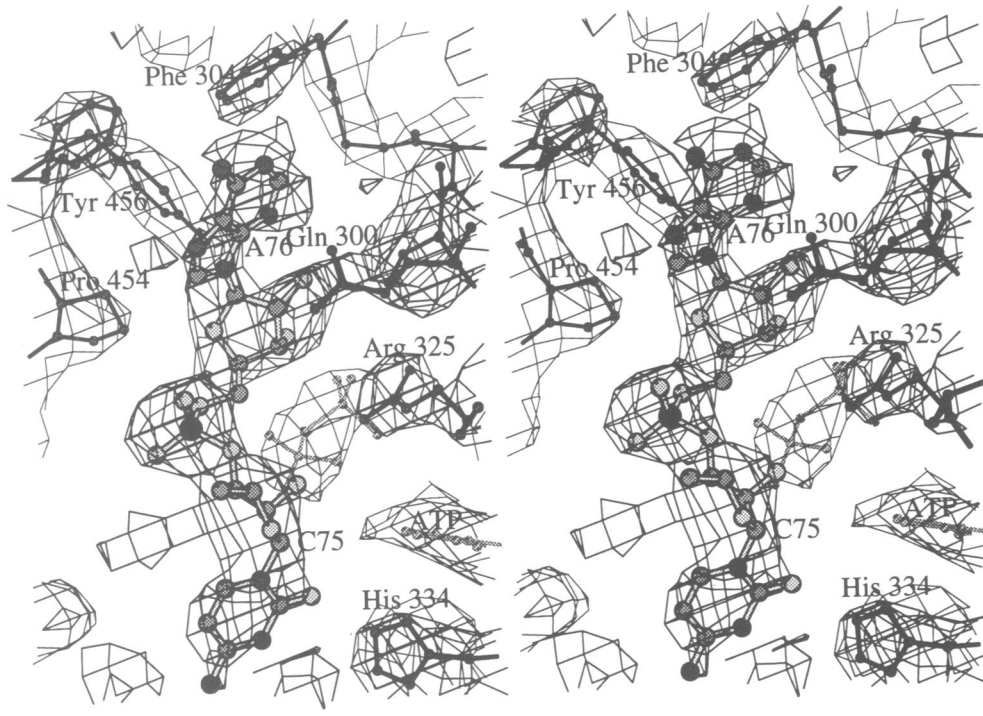

Fig. 3. Electron density map in the CCA region of the tRNA. The density shown results from a $2F_{obs}-F_{calc}$ synthesis and is contoured at the 1.0σ level.

making hydrogen bonds with the ribose of C74. The benzene ring of Phe304 is parallel to the adenine base of A76, with a partial stacking of the two bases.

The 3′ hydroxyl group of the terminal adenosine of tRNA is close to the α-phosphate of ATP, with which it can form hydrogen bonds before the fixation of the amino acid. A C2′ endo conformation of the sugar ring favors these contacts and puts the 3′ hydroxyl group in a favorable position to pick up the amino acid from the aspartyl-adenylate.

ATP or AMPPcP binding produces a large conformational change of the CCA acceptor arm which extends to the third base pair of the acceptor stem (Cavarelli *et al.*, 1993). In the absence of ATP, the adenosine of nucleotide A76 occupies the ATP binding site. A full description of the conformational changes at the tRNA level upon ATP binding will be presented elsewhere.

Amino acid binding pocket

A pocket of the appropriate size for locating an aspartic acid molecule extends the ATP binding site right after the α-phosphate. The access to it is blocked when the ATP is in place, indicating that the reaction is ordered and that the amino acid has to enter the active site first. In the electron density map of crystals soaked with the aspartic acid and ATP, this region shows density into which a complete aspartyl-adenylate molecule can be built. The electron density extends to the ribose of A76, so that it is also compatible with aminoacylated tRNA, the final product (Figure 4A). The residual electron density at the location of the β- and γ-phosphates is much weaker than for the α-phosphate, indicating that most, but not all, of the ATP has been converted to AMP or aspartyl-adenylate. Where complete ATP is left, ATP may have replaced AMP after completion of the reaction, or the reaction with the amino acid may not have taken place. In favor of the first hypothesis is the presence of a large excess of ATP in the mother liquor of the crystals. In any case, the observed electron density shows that at least the first step of the aminoacylation reaction has taken place in most crystal sites, thus confirming the enzymatic activity of the crystallized synthetases in the presence of tRNA. It is worth noting that the crystal structure of the aspartyl-tRNA synthetase from *Thermus thermophilus* complexed with the adenylate substrate, solved recently in our group (Poterszman *et al.*, manuscript in preparation), reveals an aspartyl-adenylate molecule in exactly the same conformation. The peptide group of the aspartyl-adenylate molecule is hydrogen bonded to Asp342 and Ser481. The side chain of Asp342 interacts through a water molecule with the amino group. This water molecule is not seen in our present electron density map but appears in the structure of the aspartyl-tRNA synthetase from *T.thermophilus* complexed with the adenylate substrate. Sequence alignments show that the residue at the position of Asp342 is acidic in all class II enzymes except for *E.coli* HisRS and AlaRS.

The side chain functional group of the aspartic acid substrate is specifically recognized by the enzyme. It is bonded on one side to Gln303 and Arg485, and on the other to the main chain amine group of Gly526. The amino acid substrate is inserted into a pre-existing network of interactions formed by all these residues, like the cascade of hydrogen bonds or salt bridges between Gln303, Arg485, Glu344, Lys306, Gln307 and Asp342. These residues are all strictly invariant in AspRS and the mutation of any of them renders the enzyme inactive. Another example is the main chain hydrogen bond 526 NH...O 481, at the end of the third and fourth strands of the anti-parallel β-sheet. A local distortion of the β-sheet at this place weakens the NH...O bond and enables a reorientation of the NH group towards the amino acid carboxylate. This distortion is achieved by a direct interaction, two residues away from the NH...O bond, between CO 524 and the hydroxyl group of Tyr470. This tyrosine is on the fifth strand and has to

Table II. Interatomic contacts in the active site region

Protein ... AMP (or ATP) and Mg^{2+}		
Phe 338	...	Adenine (stacking)
Arg 531	...	Adenine (stacking)
Met 335 NH	...	N1
Met 335 CO	...	N6
Arg 531 Nη	...	O2′
Ile 479 CO	...	O3′
Gly 528 NH	...	O3′
Arg 325 Nη	...	$O_P\alpha$
Arg 531 Nη	...	$O_P\gamma$
Asp 471 Oδ	...	Mg^{2+}
Glu 478 Oε	...	Mg^{2+}
Ser 481 Oγ	...	$O_P\beta$
ATP $O_P\beta$	...	Mg^{2+}
Protein ... amino acid		
Asp 342 Oδ	...	Asp NH[a]
Ser 481 Oγ	...	Asp O
Ser 481 CO	...	Asp Oδ1
Arg 485 Nη1	...	Asp Oδ1
Arg 485 Nη2	...	Asp Oδ2
Gly 526 NH	...	Asp Oδ1
Gln 303 Nε	...	Asp Oδ2
Protein ... acceptor end of tRNA		
Phe 304	...	A76 (partial stacking)
Ser 280 Oγ	...	N6
Glu 281 CO	...	N6
Gly 283 NH	...	N7
Gln 300 Nε	...	O2′
Ser 301 Oγ	...	O2′
Tyr 456 Oη	...	O4′
His 334 Nε	...	C75 O2
Ser 284 Oγ	...	O2′
Ser 329 Oγ	...	C74 N4
Ser 329 Oγ	...	N3
Glu 327 Oε	...	O2′
tRNA ... AMP/ATP		
A76 O3′	...	OPα
C75 O2	...	OPγ

Two atoms are assumed to be in direct interaction when they are separated by <3.5 Å. A dash indicates that atoms of the ribose, O_P are phosphate oxygens. Class II invariant amino acids are in boldface type, those conserved only in the AspRS sequences are in italics (see Figure 6).

[a]This is included even though the interatomic distance is >3.5 Å. The importance of Asp342 is stressed by its invariance and by the complete loss of enzymatic activity upon mutation. The interaction is water-mediated in the case of the adenylate and probably direct for the initial position of the amino acid substrate.

reach over the fourth strand at a place devoid of side chains (Gly482). Clearly, all these pre-existing interactions stabilize the environment of the substrate in the correct conformation, so that it is ready to accept an aspartic acid molecule (and nothing else) in the correct orientation. They may also enable their ultimate release with the minimum expense of energy.

All the residues mentioned in this section, except those interacting through main chain atoms, are strictly invariant within the AspRS family. Arg485 is essential for the recognition of the amino acid. Significantly, among the aligned sequences of class II, an arginine at this position is also found only in the closely related AsnRS. The discrimination between Asn and Asp is thus presumably achieved by the side chain of residue 303, a glutamine in the aspartic acid system and an aspartic acid in the asparaginyl system. In LysRS, which also belongs to the same subclass, side chain-specific recognition is also achieved by the change of Arg485 into a glutamic acid. It illustrates the conservation of the proposed model for amino acid subclass recognition in which a single change in the binding pocket triggers a switch of specificity. The correct positioning of the side chain of Arg485, at the top of the β-sheet, is incompatible with any protruding side chain at position 524 on the neighboring β-strand. Residue 524 is indeed a glycine in all class II aaRS. A small side chain (Gly or Ala) is also necessary at position 526 to make room for the aspartic acid substrate.

In conclusion, the amino acid selection, which can be generalized to class II synthetases, is achieved in a cavity mapped by side chains of amino acids conserved in all synthetases specific for a given amino acid. They establish a complex network of interactions which specifically recognizes, positions and activates the correct amino acid for the subsequent enzymatic reaction.

Site-directed mutagenesis

The molecular model of substrate binding and catalysis presented here is consistent with the site-directed mutagenesis investigations performed on AspRS. The target amino acids were chosen according to their conservation in the class II synthetases and their proximity to any of the substrates. Each selected position was substituted by several amino acids to modulate its interaction potentialities. The purified mutated proteins were tested for their catalytic properties and substrate binding capacities. The most significant results are summarized in Table III. They should be examined in the light of the residue conservation shown in Figure 6.

The substitution of residues in close contact with ATP reduces, and in most cases suppresses, the enzyme activity and often affects the K_m value for ATP. It is worth noting that in all cases changes of K_m values for ATP are coupled with variations in the aspartic acid binding properties. As a whole, the observed effects completely support the involvement of most class II-specific residues in ATP binding and correlate with the crystallographic observations: Arg325 and Arg531 on one side, Asp471 and Glu478 on the other, are indeed essential. Mutation of the two other residues in contact or in close vicinity to the ATP adenine base (Phe338 and Gly528) has a significant but less dramatic influence on the enzyme activity.

Mutation of any of the residues involved in the hydrogen bond network running from Gln303 to Asp342, through Arg485, Glu344 and Lys306, is lethal to the enzyme. A similar drastic effect is observed when any side chain, even alanine, is introduced at the position of Gly526, close to the amino acid substrate. In general, mutations at these positions have a rather significant effect on amino acid binding as well as on both enzyme activities. Inactivation of the acylation reaction is obviously related to a modification of the interaction network with the activated amino acid. Interestingly, most of these mutated proteins were only affected in the binding of Asp and not of ATP, in contrast to what was observed by the mutation of residues in contact with ATP where both binding parameters were modified. This strongly suggests an ordered ligand binding mechanism (the presence of ATP on the enzyme being a prerequisite for aspartic acid binding), a hypothesis consistent with previous observations showing that aspartic acid does not bind to AspRS in the absence of ATP (D.Kern, unpublished data).

At the level of the acceptor stem of the tRNA, residues potentially interacting with the CCA and the discriminant

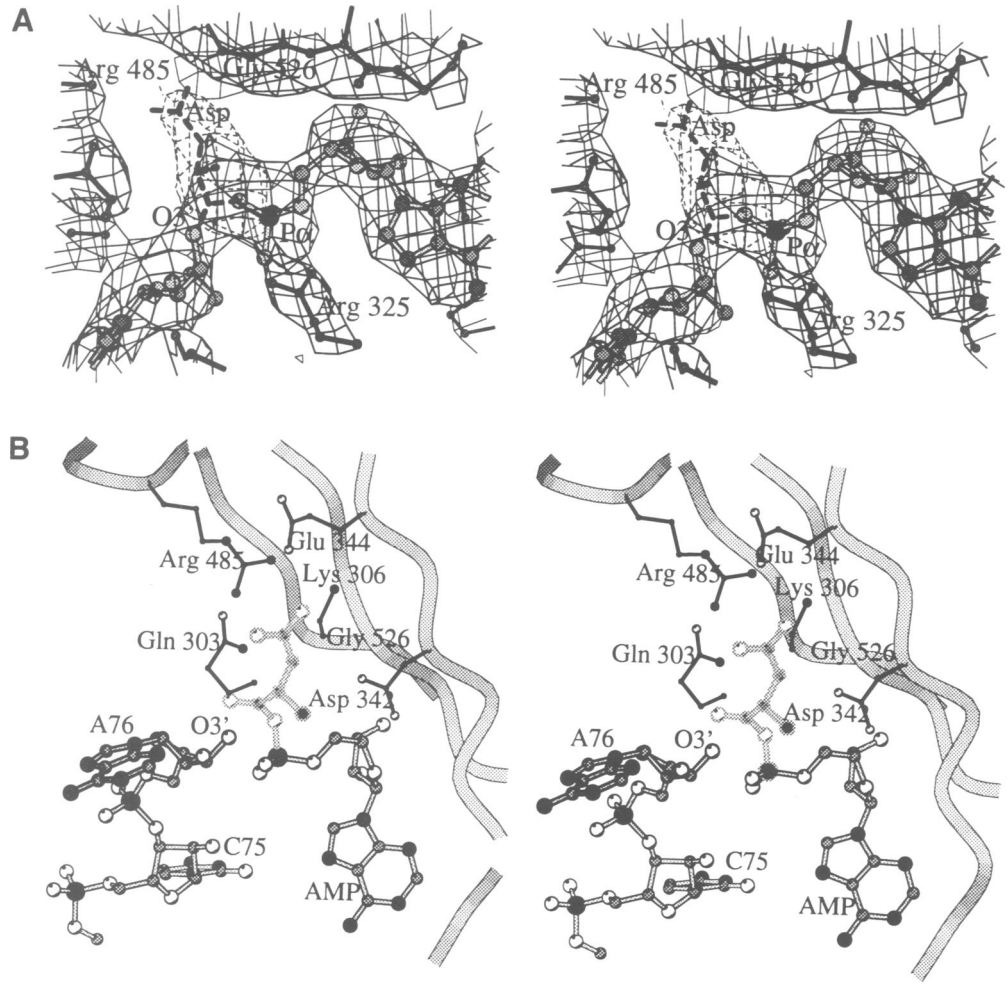

Fig. 4. (**A**) Electron density in the active site. The aspartic acid substrate (dashed) is bonded either to O3′ of ribose 76 of the tRNA or to the α-phosphate of AMP. Density from a $2F_{obs}-F_{calc}$ synthesis contoured at the 1.2σ level. Density in the aspartic acid region appears at a lower contour level or in a difference map ($F_{obs}-F_{calc}$ synthesis). Such a map, limited to this region, is shown at the 2σ level (dashed line). Both maps were calculated with phases from a model that does not include the aspartic acid substrate at any stage of the structure determination. (**B**) The main interactions of the amino acid substrate. The amino acid is shown in light grey, bonded to AMP (adenylate).

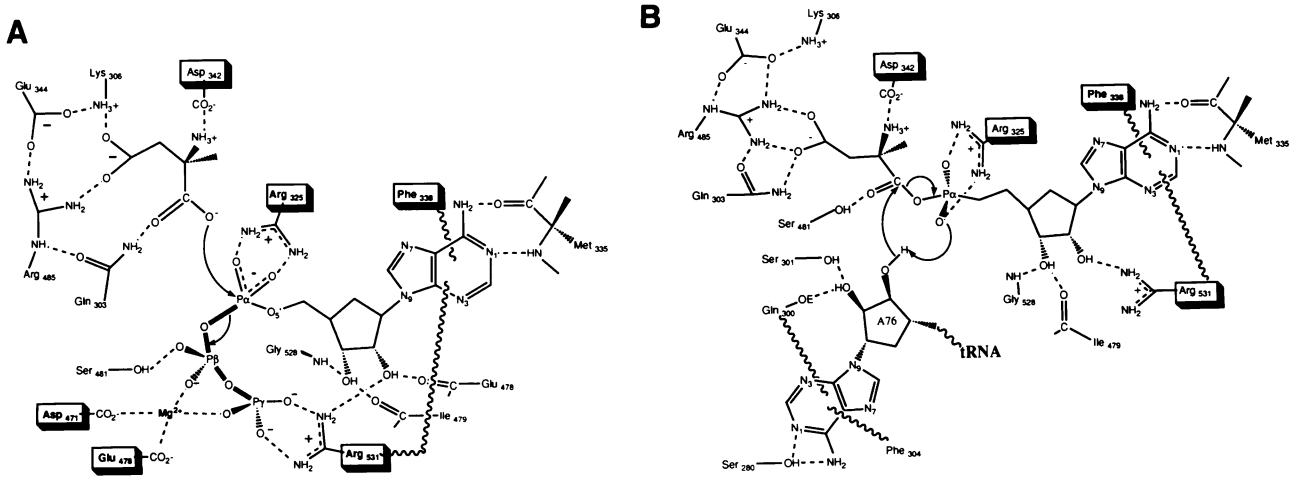

Fig. 5. The two steps of the aminoacylation reaction. (**A**) Amino acid activation with formation of the aspartyl-adenylate and release of pyrophosphate. The amino acid substrate is shown in a postulated initial position. (**B**) Amino acid transfer to the ribose of the 3′ end adenosine of tRNA. The interactions are deduced from the crystal structure. The boxes contain residues strictly or functionally conserved in class II aaRS.

base have been changed. In all cases a drastic decrease of the tRNA charging activity is observed with no effect on the amino acid activation step. Ser301, which interacts directly with the ribose, cannot be changed without a drastic loss of activity. Of particular importance are Glu327 and His334, which are in contact with positions 74 and 75 of

Table III. Catalytic properties of mutated aspartyl-tRNA synthetases

Protein	tRNA acylation (sec^{-1})	Pyrophosphate exchange (sec^{-1})	K_m ATP (μM)	K_m Asp (mM)	K_d $tRNA^{Asp}$ (M)
Native AspRS	0.83	27	30	2.5	$3\ 10^{-8}$
Mutations with effect on ATP binding					
Arg 325 Lys	0	10.69	10 000[a]	80	$6.6\ 10^{-8}$
Arg 325 His	0	0	–	–	ND
Arg 325 Gln	0	0	–	–	ND
Arg 325 Asn	0	0	–	–	ND
Arg 325 Leu	0	0	–	–	ND
Phe 338 Ala	0.15	3.12	6 660	15	ND
Phe 338 Leu	0.10	0.82	6 450	10	$1.0\ 10^{-8}$
Phe 338 His	0.15	16.16	555	14	$5.0\ 10^{-8}$
Asp 471 Ala	0	0	–	–	$5.0\ 10^{-8}$
Asp 471 Asn	0	1.28	ND	43.5	ND
Asp 471 Glu	0.0073	6.09	1 750	19.6	ND
Glu 478 Ala	0	0	–	–	ND
Glu 478 Asp	0	0	–	–	$3.0\ 10^{-8}$
Glu 478 Gln	0	0	–	–	ND
Ser 481 Ala	0	0	–	–	$4.0\ 10^{-8}$
Ser 481 Thr	0.13	0.27	400	14.3	ND
Ser 481 Cys	0	0	–	–	ND
Gly 528 Ala	0.50	6.34	3 570	10	ND
Arg 531 His	0	0	–	–	$2.3\ 10^{-8}$
Arg 531 Lys	0	0	–	–	$2.8\ 10^{-8}$
Arg 531 Gln	0	0	–	–	ND
Arg 531 Asn	0	0	–	–	ND
Mutations with effect on amino acid binding					
Gln 303 Ala	0	2.30	NM	47	ND
Gln 303 Glu	0	2.08	NM	56	ND
Gln 303 Asn	0	3.11	NM	166	$13\ 10^{-8}$
Lys 306 Arg	0	0	–	–	$4.4\ 10^{-8}$
Lys 306 Thr	0	0	–	–	ND
Gln 307 Ala	0.0029	0.82	105	55.5	$7.0\ 10^{-8}$
Gln 307 Glu	0.358	19.36	75	9.1	ND
Gln 307 Asn	0	2.43	ND	62.5	ND
Asp 342 Ala	0	0	–	–	ND
Asp 342 Glu	0.012	5.27	133	55.5	$5.0\ 10^{-8}$
Asp 342 Asn	0	0	–	–	ND
Glu 344 Ala	0	0	–	–	ND
Glu 344 Asp	0.19	21.91	118	18	$8.0\ 10-^{8}$
Glu 344 Gln	0	0	–	–	ND
Arg 485 Ala	0	0	–	–	$5.0\ 10^{-8}$
Arg 485 His	0	11.02	NM	30	ND
Arg 485 Lys	0	0	–	–	ND
Gly 526 Ala	0	10	8 300[a]	58 800	$4.5\ 10^{-8}$
Mutations with effect on tRNA binding					
Ser 280 Ala	0.086	33.75	13	18	$3\ 10^{-8}$
Gln 300 Glu	0.046	20.52	9	8.9	$5.5\ 10^{-8}$
Gln 300 Ala	0.035	9.83	12	7.14	$2.5\ 10^{-8}$
Ser 301 Ala	0.01	15.5	57.5	59	$5.0\ 10^{-8}$
Phe 304 Ala	0.087	13.22	6	10	$3.0\ 10^{-8}$
Glu 327 Gln	0.037	6.5	121	111	$1.35\ 10^{-8}$
Glu 327 Ala	0.055	4.53	125	30	$2.0\ 10^{-8}$
Ser 329 Ala	0.096	41.44	26	3.2	$12\ 10^{-8}$
His 334 Arg	0.21	27	120	50[b]	$24\ 10^{-8}$
His 334 Lys	0.062	0.62	290	50[b]	$27\ 10^{-8}$
His 334 Asn	0.15	15.7	285	150[b]	ND
His 334 Gln	0.82	2.7	1 000	4 200[b]	ND
Tyr 456 Phe	0.44	17.36	27	25	7.0 10−8

The aminoacylation reactions were performed at the non-saturating concentration of 10^{-4} M aspartic acid; K_m for ATP were measured in the charging reaction; when not specified, K_m values for aspartic acid were determined in the pyrophosphate exchange reaction; K_d for $tRNA^{Asp}$ was measured by filtration assay according to Yarus and Berg (1967).

[a]Determined in the pyrophosphate exchange reaction.

[b]Determined in the aminoacylation reaction.

NM, not measurable; ND, not determined.

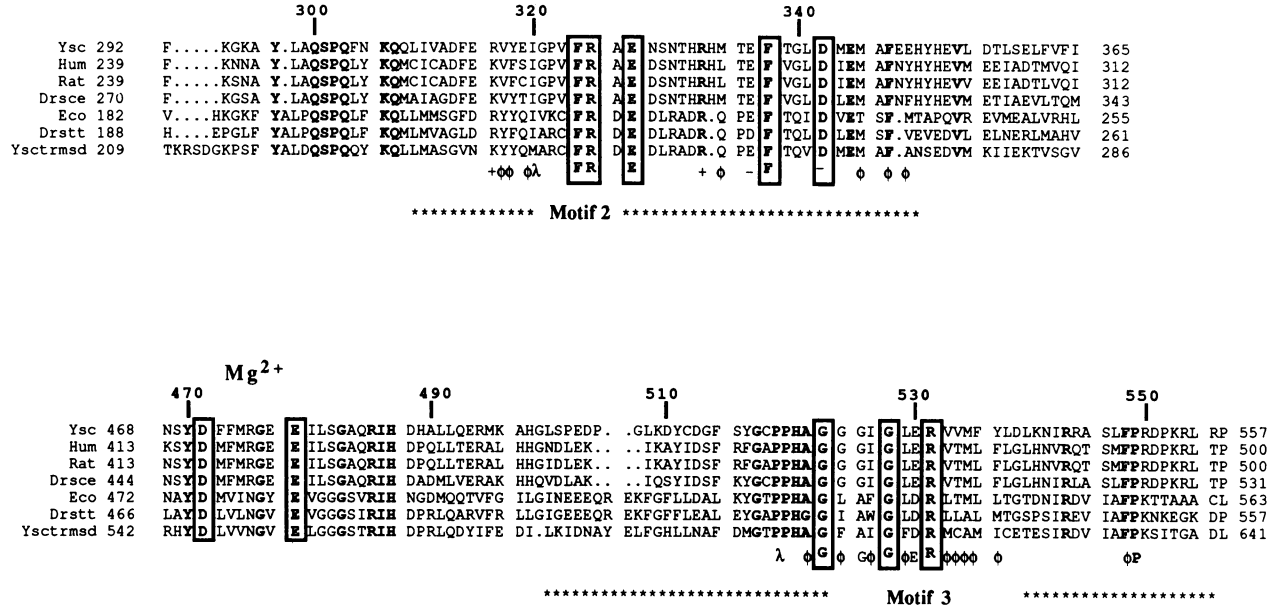

Fig. 6. Sequence alignment of AspRS from different eukaryotic and prokaryotic organisms in the active site region. Ysc, *Saccharomyces cerevisiae*; Hum, Human; Rat, rat liver; Drsce, *Caenorhabditis elegans*; Eco, *E.coli*; Drstt, *T.thermophilus*; Ysctrmsd, *S.cerevisae* mitochondrial. Two of the three conserved motifs of class II synthetases are indicated. Residues in bold are conserved in the AspRS system. The boxes contain residues strictly or functionally conserved (e.g. Asp/Glu) in class II. The sequence numbers are those of Ysc AspRS. The bottom line contains symbols for amino acids strongly conserved: λ, small amino acids (P, G, A, S, T); ϕ, hydrophobic or aromatic residues (M, L, V, C, F, Y, W); +, positively charged residues (H, K, R); −, negatively charged residues (D, N, E, Q).

the tRNA. Mutation of these strongly conserved motif 2 residues modifies the activity of both reaction steps as well as the K_m values for ATP and the amino acid. These effects obviously reflect a more complex function than CCA binding alone. Mutation of Gln300 and Phe304, which are in contact with adenine 76, significantly affect the acylation reaction but to a lesser extent. One single remarkable exception is Tyr456: the crystal structure clearly shows a direct interaction with the ribose of A76, thus suggesting a role in the positioning of this key element of the reaction. However, the mutation of Tyr to Phe is almost without effect on the enzyme activity. The lack of conservation of this residue among AspRS enzymes confirms the accidental character of this interaction.

Despite their critical role in aminoacylation, individually all these residues contribute only weakly to the total tRNA−enzyme binding energy, as shown by the rather small K_d changes of the inactive enzymes. This might be compared with the important affinity changes observed when interactions with the anticodon are affected (Martin *et al.*, in press). Additional CCA binding energy (not revealed by K_d measurements) may exist, assigned to the stability of this part of the molecule in the acylation transition state.

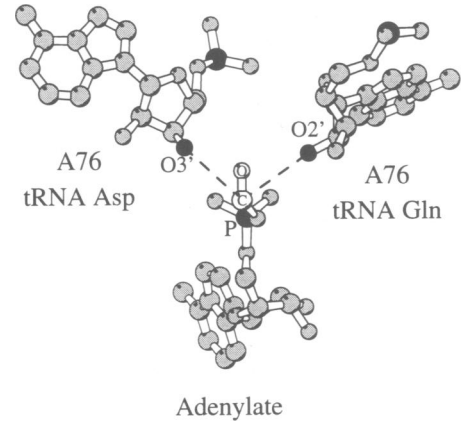

Fig. 7. Aminoacylation in class I and II aaRS: relative positions of the terminal adenosines versus the adenylate moieties. The orientations result from the superposition of the two AMP groups of GlnRS and AspRS structures (for the aminoacyl-adenylate only the AMP and the α-carbonyl group of the amino acid is shown). In class I GlnRS, the terminal adenosine of tRNA is on the right-hand side and the amino acid is transferred to the 2′ hydroxyl of the ribose. In class II AspRS, it is on the left-hand side and the initial attachment site is the 3′ hydroxyl group.

Discussion

The aminoacylation reaction

The presently available crystal structures in the yeast aspartic acid system give some insight into each step of the aminoacylation reaction. The following pathway can be proposed which takes into account all observed contacts, as well as the results of site-directed mutagenesis (Figure 5).

(i) Prior to the first step of the reaction, aspartic acid and ATP bind to their respective pockets. ATP adopts the bent conformation with its γ-phosphate pointing towards Arg531 (Figure 5A). At this stage, the aspartic acid substrate is slightly shifted from the position observed in the adenylate. Asp342 may play an essential role in positioning the amino acid via direct interaction with the amino group, and in activating the nucleophilic character of the α-carboxylate attacking group of the amino acid. Lys306, Glu344, Arg485 and Gln303 are responsible for the correct positioning of the α-carboxyl group. Nucleophilic attack of the α-phosphate does not require significant movements of the substrates. The pivotal position of the α-phosphate is maintained by the class II invariant Arg325, which stabilizes the penta-coordinated intermediate. Hydrolysis of the phosphate bond, followed by the release of the pyrophosphate group, is activated by the magnesium ion and Arg531. All these amino acids are

strictly conserved in the aspartic system. They are responsible for maintaining the local environment necessary for the activation of the amino acid. Mutations of these residues have a dramatic effect on the first step of the reaction.

(ii) The resulting adenylate is then ideally located, underneath the terminal ribose of tRNA, for the second step of the reaction. A nucleophilic attack by the 3′ hydroxyl group of the sugar moiety can take place on the carboxylic group of the adenylate (Figure 5B). One of the two free oxygen atoms of the α-phosphate attracts the proton from the 3′ hydroxyl of A76, forming a cyclic intermediate. No other chemical group in the vicinity is able to play this role. A similar mechanism has been recently postulated for the glutaminyl system (Perona *et al.*, 1993) and *Eco*RV endonuclease (Jeltsch *et al.*, 1993). An intricate network of interactions with many residues helps to stabilize the substrates. Mutation of these residues results in a complete inactivation of the acylation capacity of AspRS and has a strong effect on the binding of the aspartic acid (Table III).

aaRS classification: a similar catalytic mechanism within two different frameworks

When comparing class I and II active sites the best reference is the coenzyme. Figure 7 shows the relative positions of the adenylate and acceptor adenosine substrates as a result of the superposition of AMP moieties as seen in GlnRS or TyrRS (class I) and AspRS (class II, this study). The adenosine ends of $tRNA^{Gln}$ and of $tRNA^{Asp}$ occupy different sides of the adenylate. The sugar pucker of the terminal adenosine is C2′ endo for $tRNA^{Asp}$ and C3′ endo for $tRNA^{Gln}$. In this conformation, the 3′ hydroxyl group of $tRNA^{Asp}$ is stereochemically positioned for attack on the carboxyl group of the adenylate, whereas for $tRNA^{Gln}$ only the 2′ hydroxyl group can perform this job. In both classes, one of the free oxygen atoms of the α-phosphate acts as proton attractor. The amino acid pocket is lined with highly conserved amino acid-specific residues. Residues binding the CCA end show a similar conservation (Delarue and Moras, 1993). These comparisons explain the functional differences observed in the two classes and suggest that the situations observed in AspRS and GlnRS are most certainly representative of their respective classes. The fact that class-conserved residues are implicated in the proper positioning of the substrates supports this view and emphasizes the importance of two different chiral centers implicated in the terminal acceptor ribose.

Despite the different structures, the two aminoacylation mechanisms present striking similarities. We will only point out three remarkable features: (i) in the first step of the reaction the amino acid substrate is positioned by an interaction between the peptidic amino group and the side chain of a conserved acidic residue; (ii) a magnesium ion is bound to the labile pyrophosphate group and most likely contributes to the hydrolysis reaction; and (iii) for the transfer of the amino acid to the tRNA, a free oxygen of the α-phosphate serves as proton attractor to the attacking 2′ or 3′ hydroxyl group of the terminal adenosine. Thus, the two classes of aaRS illustrate how a similar catalytic mechanism within aaRS can be accomplished by two totally different active site frameworks.

Materials and methods

Crystal structure analysis

Crystals of the yeast $tRNA^{Asp}$–AspRS complex used for this study were grown, following the procedure described elsewhere (Ruff *et al.*, 1988), as plates of typically 0.4 × 0.8 mm in their largest dimensions, with a thickness varying between 0.06 and 0.20 mm. The native data were collected at the EMBL synchrotron outstation at DESY in Hamburg with the imaging plate system locally developed by J.Hendrix and A.Lentfer. Data processing was performed using the MOSFLM package. Native data, collected at a short wavelength (1.0 Å), were derived from a collection of 310 oscillations from 22 crystals. Crystals belong to space group $P2_12_12$ with unit cell parameters a = 210.2 Å, b = 146.2 Å, c = 86.1 Å (Ruff *et al.*, 1991). They contain two monomeric molecules per asymmetric unit, related by a 2-fold non-crystallographic symmetry. Complexes with AMPPcP, ATP or ATP and aspartic acid were obtained by soaking the native crystals at pH 7.4 in the presence of 80% ammonium sulfate. The soaking conditions were: (i) AMPPcP 0.2 mM, $MgCl_2$ 5 mM, 6 h; (ii) ATP 2.5 mM, $MgCl_2$ 5 mM, 12 h; (iii) ATP 5 mM, aspartic acid 5 mM, $MgCl_2$ 5 mM, 12 h. The corresponding data were collected at LURE at a wavelength of 0.9 Å using a MARResearch imaging plate system. Data processing was done using the MOSFLM package included in the CCP4 suite (CCP4, 1979). The ATP data set used seven crystals with an oscillation range between 0.6° and 1.0°, an exposure time of 6 min and a crystal-to-plate distance of 286 mm; 10 crystals were used for the ATP and aspartic acid data set and six crystals were used for the AMPPcP data set, with experimental conditions similar to the ATP data set. Data scaling and analysis were performed using the CCP4 package.

The refinement of the native structure has been reported elsewhere (Cavarelli *et al.*, 1993). For the other structures the protocol used consisted of cycles of conventional crystallographic coordinate refinement using Xplor (Brünger, 1988) and model building into electron density maps using FRODO (Jones, 1978) and O (Jones and Thirup, 1986). Solvent molecules have not yet been included. The first 65 residues of each monomer of AspRS are not visible in the maps and are at least partly disordered in the crystals. It has been shown that the first 90 residues can be deleted without affecting the enzymatic activity of the enzyme (Eriani *et al.*, 1991). The structures differ mainly at the active site level. In the native structure, the conformations are different in the two subunits. One subunit, where the CCA end of tRNA occupies its functional location, contains clear electron density where a complete AMP molecule can be fitted, although the crystals were grown in the absence of ATP in the mother liquor. In the other subunit, this site is partially occupied by the terminal adenosine of tRNA as a result of a conformational change which extends up to the third base pair of the acceptor stem. Soaking of AMPPcP or ATP into the crystals leads to fully symmetrical dimers.

Site-directed mutagenesis

Bacterial strains and plasmids. CJ236 [*dut, ung, thi, rel* A, pCJ105 (*Cm*^{r})] was the host strain for the preparation of uracil-containing DNA.

MV1190 [Δ(*lac-pro* AB), *thi, sup* E, Δ(*sr*1-*rec* A)306::Tn*10* (*Tet*^{r}) (F′: *tra* D36, *pro* AB, *lac* I^{q}ZΔM15)] was used as a recipient after the Kunkel procedure of mutagenesis (Kunkel, 1985).

TGE900 [F^-, *su, ilv, bio,* (λ *cI*857, Δ*Bam*ΔHI)] was the host strain of pTG908 harboring the *APS* gene. It was kindly provided by M.Courtney from Transgene. This plasmid allows the high-efficiency expression of the APS gene after heat induction (Courtney *et al.*, 1984).

Enzymes, chemicals, nucleic acids and standard procedures

Restriction enzymes, T4 DNA ligase, T4 DNA polynucleotide kinase and T4 DNA polymerase were obtained from Boehringer Mannheim. T7 DNA polymerase was purchased from Pharmacia. All enzymes were used according to the manufacturer's instructions. [α-^{35}S]dATP, [γ-^{32}P]ATP were acquired from Amersham, and [^{14}C]L-aspartic acid from the Commissariat à l'Energie Atomique (Saclay, France). Progel™-TSK column HA-1000 used for mutated AspRS purification was obtained from Supelco. Standard procedures were used for plasmid preparation and DNA manipulations (Maniatis *et al.*, 1982).

Oligonucleotide-directed site-specific mutagenesis

Mutagenic primers were synthesized on a fully automated DNA synthesizer (Applied Biosystem 381A DNA). Mutagenesis of single stranded DNA from bacteriophage M13mp18-*APS* was performed according to the method described by Kunkel (1985). Mutated AspRS genes were characterized by DNA sequencing and were subcloned as a *Sac*I–*Mlu*I DNA fragment into pTG908-*APS* opened at the same sites.

Preparation of pure mutated AspRS

The *AspRS* gene contained in the recombinant plasmid pTG908-*APS* was overexpressed in the TGE900 strain, and crude extracts were prepared (Eriani *et al.*, 1991). Purification of the over-expressed AspRS proteins was performed in one fractionation step by HPLC on a hydroxyapatite column (HA-1000): 4 ml of the 105 000 *g* crude extract were loaded, at a flow rate of 0.5 ml/min, on the column equilibrated in 275 mM potassium phosphate pH 7.6, 0.01 mM $CaCl_2$. The column was washed at 1 ml/min with 25 ml of the equilibration buffer and protein eluted by raising the phosphate concentration linearly for 20 ml to a final concentration of 700 mM. The fractions containing the enzyme (~3 ml) were pooled, concentrated on a Millipore PM 30 Centricon filter, washed twice with 1 ml of 50 mM Tris–HCl pH 8, 1 mM $MgCl_2$, 0.1 mM EDTA, 5 mM β-mercaptoethanol and stored in the same buffer containing 60% glycerol.

Measurement of kinetic parameters

$tRNA^{Asp}$ aminoacylation k_{cat} and K_m values were established as described (Eriani *et al.*, 1991).

The K_d of AspRS for ^{32}P-labeled $tRNA^{Asp}$ was determined by the nitrocellulose filtration method (Yarus and Berg, 1967): the binding mix (100 μl) was 3 nM in [^{32}P]$tRNA^{Asp}$ (~3×10^{-5} c.p.m. per pmol), 100 mM HEPES pH 7.5, 10 mM $MgCl_2$, 30 mM KCl and various enzyme concentrations extending from 10^{-8} to 10^{-6} M. The filters (pore size, 0.22 μm; diameter, 25 mm) were washed twice with 0.5 ml 50 mM potassium phosphate pH 5.5 and 50 mM $MgCl_2$, dried and counted.

Acknowledgements

These results were presented at the 15th International tRNA workshop (Cap d'Adge, France, May 30–June 4, 1993). We thank R.Fourme and the staff of LURE (Orsay, France), and K.Wilson and the staff of the EMBL outstation at the DESY (Hamburg, Germany) for their support during data collection. We thank A.Poterszman and M.Delarue for unpublished data on the AspRS *Thermus thermophilus* structure, C.Florentz and R.Giegé for making available to us their bibliographic database, and D.Logan for careful reading of the manuscript. We are grateful to T.A.Steitz for the coordinates of the complex $tRNA^{Gln}$–GlnRS. This work was supported by grants from the Human Science Frontier Program and the EEC Science Program.

References

Bossemeyer,D., Engh,R.A., Kinzel,V., Ponstingl,H. and Huber,R. (1993) *EMBO J.*, **12,** 849–859.

Brick,P., Bhat,T.N. and Blow,D.M. (1989) *J. Mol. Biol.*, **208,** 83–98.

Brünger,A. (1988) *J. Mol. Biol.*, **203,** 803–816.

Brunie,S., Zelwer,C. and Risler,J.L. (1990) *J. Mol. Biol.*, **216,** 411–424.

Burbaum,J., Starzyk,R.M. and Schimmel,P. (1990) *Proteins*, **7,** 99–111.

Carson,M.K. (1991) *J. Appl. Crystallogr.*, **24,** 958–961.

Cavarelli,J., Rees,B., Ruff,M., Thierry,J.C. and Moras,D. (1993) *Nature*, **362,** 181–184.

CCP4 (1979) *The SERC Collaborative Computing Project N°4, a Suite of Programs for Protein Crystallography*. Daresbury Laboratory, Warrington, UK.

Courtney,M. *et al.* (1984) *Proc. Natl Acad. Sci. USA*, **81,** 669–673.

Cusack,S., Berthet-Colominas,C., Härtlein,M., Nassar,N. and Leberman,R. (1990) *Nature*, **347,** 249–255.

de Prat Gay,G., Duckworth,H.W. and Fersht,A.R. (1993) *FEBS Lett.*, **318,** 167–171.

Delarue,M. and Moras,D. (1993) *Bioessays*, **15,** 675–685.

Eriani,G., Delarue,M., Poch,O., Gangloff,J. and Moras,D. (1990) *Nature*, **347,** 203–206.

Eriani,G., Prevost,G., Kern,D., Vincendon,P., Dirheimer,G. and Gangloff,J. (1991) *Eur. J. Biochem.*, **200,** 337–343.

Fersht,A.R. (1987) *Biochemistry*, **26,** 8031–8037.

Fersht,A.R., Knill-Jones,J.W., Bedouelle,H. and Winter,G. (1988) *Biochemistry*, **27,** 1581–1587.

Hountondji,C., Dessen,P. and Blanquet,S. (1986) *Biochimie*, **68,** 1071–1078.

Jeltsch,A., Alves,J., Wolfes,H., Maas,G. and Pingoud,A. (1993) *Proc. Natl Acad. Sci. USA*, **90,** 8499–8503.

Jones,T.A. (1978) *J. Appl. Crystallogr.*, **11,** 268–272.

Jones,T.A. and Thirup,S. (1986) *EMBO J.*, **5,** 819–822.

Kraulis,P.J. (1991) *J. Appl. Crystallogr.*, **24,** 946–950.

Kunkel,T.A. (1985) *Proc. Natl Acad. Sci. USA*, **82,** 488–492.

Lapointe,J. and Giegé,R. (1991) In Trachsel,H. (ed.), *Translation in Eukaryotes*. CRC Press Inc., Boca Raton, FL, pp. 35–69.

Maniatis,T., Fritsch,E.F. and Sambrook,J. (1982) *Molecular Cloning: A Laboratory Manual*. Cold Spring Harbor Laboratory Press, Cold Spring Harbor, NY.

Martin,F., Eriani,G., Eiler,S., Moras,D., Dirheimer,G. and Gangloff,J. (1993) *J. Mol. Biol.*, in press.

Perona,J.J., Rould,M.A. and Steitz,T.A. (1993) *Biochemistry*, **32,** 8758–8771.

Rossmann,M.G., Moras,D. and Olsen,K.W. (1974) *Nature*, **250,** 194–199.

Rould,M.A., Perona,J.J., Söll,D. and Steitz,T.A. (1989) *Science*, **246,** 1135–1142.

Rould,M.A., Perona,J.J. and Steitz,T.A. (1991) *Nature*, **352,** 213–218.

Ruff,M., Cavarelli,J., Mikol,V., Lorber,B., Mitschler,A., Giegé,R., Thierry,J.-C. and Moras,D. (1988) *J. Mol. Biol.*, **201,** 235–236.

Ruff,M., Krishnaswamy,S., Boeglin,M., Poterszman,A., Mitschler,A., Podjarny,A., Rees,B., Thierry,J.-C. and Moras,D. (1991) *Science*, **252,** 1682–1689.

Schimmel,P. (1987) *Annu. Rev. Biochem.*, **56,** 125–158.

Schimmel,P. and Söll,D. (1979) *Annu. Rev. Biochem.*, **48,** 601–648.

Söll,D. (1991) *Experientia*, **46,** 1089–1096.

Yarus,M. and Berg,P. (1967) *J. Mol. Biol.*, **28,** 479–485.

Received on October 11, 1993; revised on November 11, 1993